JET–CP(98)34

H-mode Physics Studies with LHCD on JET

F X Söldner, Y Baranov, J A Dobbing, A Ekedahl,
C Gormezano, E Righi[1], P Schild.

JET Joint Undertaking, Abingdon, Oxfordshire, OX14 3EA,
[1]present address: NET Team, D-85748 Garching, Germany.

INTRODUCTION

H-modes have mostly been obtained with pre-dominant ion heating from neutral beam injection (NBI) or ion cyclotron resonance heating (ICRH) [1]. Few data exist on H-modes with electron heating schemes also being considered for ITER. H-modes with electron cyclotron heating (ECRH) had first been achieved on DIII-D [2] but no scaling studies have been carried out so far. Combined electron and ion heating from Lower Hybrid (LH) wave heating and NBI has been used in H-modes on ASDEX [3]. LH alone produced H-modes in limiter tokamak discharges on JT-60U [4]. In this paper we present the first H-modes in single null X-point plasmas with Lower Hybrid Current Drive (LHCD) as only additional power source with strongly off-axis power deposition as required in Advanced Tokamak scenarios [5]. Coupling of LH waves to H-mode plasmas, fast electron confinement and the scaling of the power threshold for L-H transitions with LHCD are discussed.

OPERATION REGIME

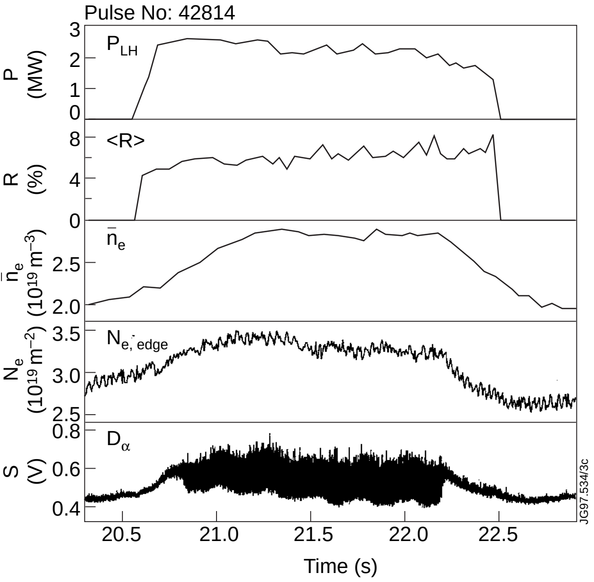

FIG.1: LHCD heated ELMy H-mode in tritium. Coupled LH power, average reflection coefficient, line averaged and edge line density and outer divertor D_α emission.

LHCD experiments on JET have focused mainly on current drive and profile control studies. The full plasma current up to 3 MA has been driven with LHCD. LH power up to 7.3 MW has been coupled into X-point plasmas well matched for low LH reflection. Recently LHCD has contributed to improve high performance regimes [6]. In these scenarios LHCD is required to provide off-axis current drive with reliable coupling under varying plasma edge conditions. The maximum power which can then be coupled with the single grill launcher on JET is limited to ~3.5 MW by the maximum sustainable electric field in the waveguides. In view of these requirements, H-modes with LHCD have been studied in the following parameter range: P_{LH} = 1.3 - 3.4 MW ($N_{\|}$ = 1.84), I_p = 1.7 - 3 MA, B_t = 1.7 - 2.9 T, n_e = 1.5 - 2.7x10^{19} m^{-3}. ELMy H-modes could be established in deuterium and tritium while in hydrogen the plasma remained in L-mode up to the highest LH power level applied. A typical H-mode with LHCD alone in tritium is shown in Fig. 1. The LHCD H-modes show small amplitude ELMs at high frequency in the range 1-2 kHz. The ELMs are only seen on the D_α emission from the outer divertor not from the main plasma. This appearance is similar to dithering ELMs with NBI heating. Line averaged and edge density increase after the onset of ELMs and decrease again after the end of the H-mode phase before the end of the LH pulse. In L-modes usually no density rise has been seen during LHCD.

COUPLING OF LH WAVES TO H-MODE PLASMAS

In ELM-free H-modes produced with NBI and ICRH on JET the coupling of LH waves often degrades due to the short density decay length in the scrape-off layer. In these conditions control of the density in front of the grill by real time control of the plasma-launcher distance or by local gas injection is required [6].

Good coupling is maintained during ELMy H-mode phases with high power NBI and also with LHCD alone (Fig. 1). The average reflection coefficient stays low in the range <R> = 3-7 %. The homogeneity across the whole grill area (0.5 m wide x 1 m high) improves in presence of the ELMs. The small amplitude/high frequency ELMs produced with LHCD reduce the sensitivity of coupling to the shape match between plasma and antenna contour.

CONFINEMENT

The LHCD power deposition profile in the H-mode discharges in deuterium and tritium was hollow with the peak located at about mid-radius (Fig. 2). This shape of the deposition profile is the same as required for current profile control in Advanced Tokamak scenarios.

The pressure and electron temperature profiles are peaking. No edge pedestal is formed in the electron temperature profile. The density profile maintains a broad shape inside the edge transport barrier and develops a pedestal during the H-mode phase. The q-profile remains

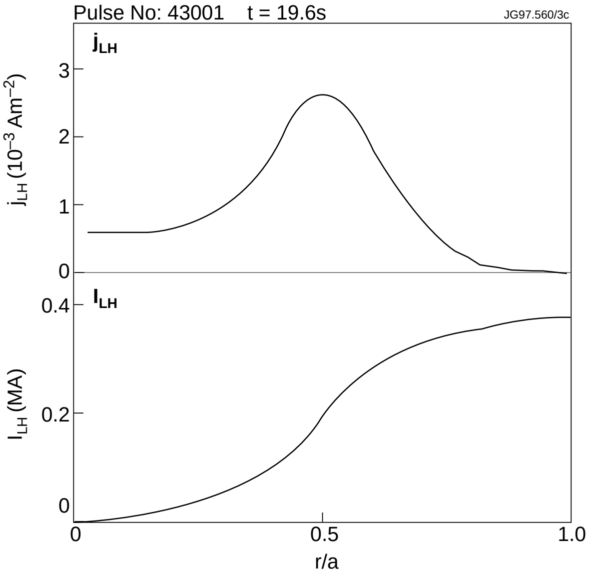

Fig.2: LHCD current deposition profile and volume integrated current profile in an ELMy H-mode tritium discharge with LHCD heating alone.

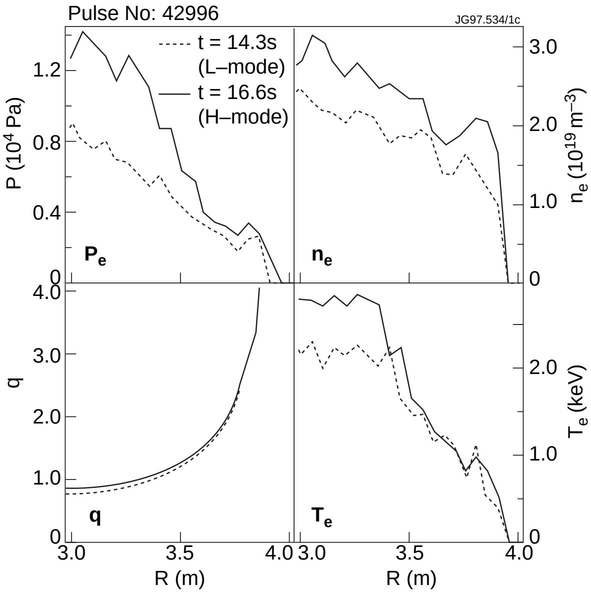

FIG.3: Radial pressure, density, q and electron temperature profiles during L- and ELMy H-mode phases with LHCD heating of a tritium discharge.

similar in L and H-mode. Central q-values stay below 1 and sawteeth persist during the ELMy H-mode phase (Fig. 3).

ELMs lead to increased losses of fast electrons rising towards the plasma boundary. This is seen from a drop in apparent ECE temperatures during the ELMy H-mode phase. The ECE emission profile with its modifications by ELMs and sawteeth is shown in Fig. 4. The depression during the ELMs (dark hatched area) aligns the ECE profile with the thermal LIDAR temperature profile. The drop can therefore be contributed to a decrease in suprathermal emission from fast electrons which enhances ECE above its thermal level during LHCD. The effect of the ELMs is much larger than the radial re-distribution during sawteeth (light hatched area). This can explain the difference in density and temperature profile evolution as discussed above.

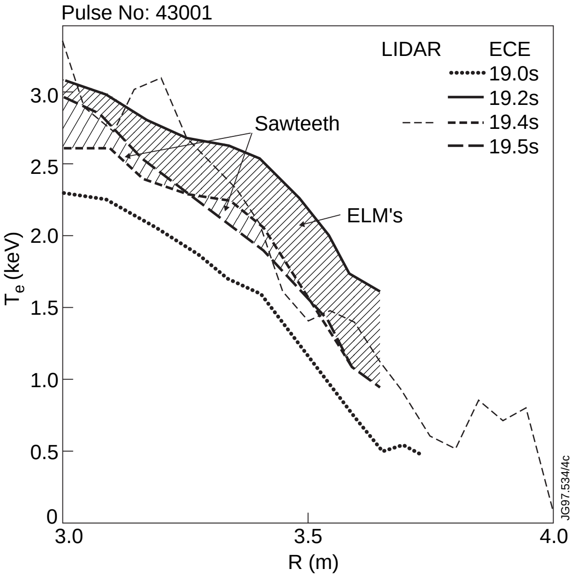

Fig.4: Electron temperature profiles as determined from Thomson scattering and ECE emission.

Global confinement remains close to L-mode with H factors typically $H^{\mathrm{ITER\ 89-P}} \approx 1.2$ in the LHCD heated dithering ELMy H-modes.

H-MODE POWER THRESHOLD

H-modes have been established with additional power input from LHCD alone above the same power threshold as required with NBI and ICRH. This has been assessed also with subsequent separate pulses of NBI and LHCD into the same discharge.

H-modes have been produced in deuterium and tritium discharges but not in hydrogen. In tritium H-modes could be achieved with an LH power input as low as 1.1 MW. The threshold power decreases with increasing isotope mass of the main ion species. This dependence is consistent with the isotope scaling found with NBI and ICRH (Fig. 6).

LHCD H-modes follow the JET scaling with an inverse linear isotope dependence [7]:

$$P_{\mathrm{th,JET}} = 0.75\, n_e^{0.75}\, B_t\, R^2\, A_{\mathrm{eff}}^{-1.08} \quad (\mathrm{MW},\ 10^{20}\mathrm{m}^{-3},\ \mathrm{T},\ \mathrm{m})$$

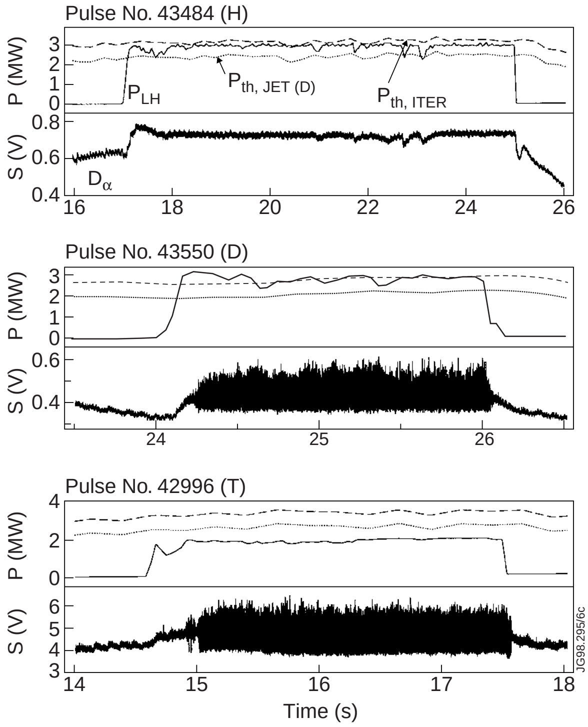

FIG.5: LHCD heated discharges in L-mode in hydrogen and in H-mode in deuterium and tritium. Threshold powers from ITER and JET(D) scalings.

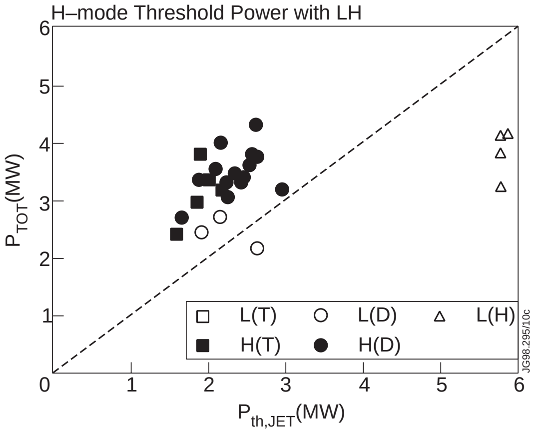

Fig.6: Total power input with LHCD into L- and H-mode plasmas versus the JET H-mode threshold power scaling including an isotope dependence

SUMMARY

For the first time H-modes have been obtained with Lower Hybrid Current Drive (LHCD) as only additional power input on JET. The power deposition profile in the H-mode discharges was strongly hollow, with the peak located at mid radius. This shape of the deposition profile is the same as required for current profile control in Advanced Tokamak scenarios.

ELMy H-modes have been established both in deuterium and tritium plasmas. Good coupling has been maintained during ELMy H-modes. ELMs lead to enhanced losses of fast electrons. The threshold power for LH-produced H-modes is comparable with the power required for L-H transitions with neutral beam (NBI) and ion cyclotron wave (ICRH) heating. It decreases with increasing isotope mass of the main ion species. LH-triggered H-modes follow the same isotope scaling as observed for NBI and ICRH.

This has implications for the understanding of the basic mechanism of the H-mode formation. Losses of LH-generated fast electrons entail a positive charging of the plasma while the opposite polarity results from fast ion losses in NBI and ICRH heated H-modes. The experimental results on JET indicate that the threshold power for the L-H transition is independent of the particle species preferentially heated and the direction of the radial electric field at the plasma edge.

REFERENCES

[1] Thomsen, K., et al., Nucl. Fusion 34, 131 (1994).

[2] Lohr, J.M., et al., Phys. Rev. Lett. 60, 2630 (1988).

[3] Söldner, F.X., et al., Nucl. Fusion 33, 333 (1993).

[4] Tsuji, S., et al., Phys. Rev. Lett. 64, 1023 (1990).

[5] Boucher, D., et al., Plasma Physics and Controlled Nuclear Fusion Research 1996 (Proc. 16th Int. Conf. Montreal, 1996), Vol. I, IAEA, Vienna (1997), 487.

[6] Ekedahl, A., et al., 12th Topical Conference on Radio Frequency Power in Plasma, Savannah (1997).

[7] Jacquinot, J., et al., this conference.